El Niño–Southern Oscillation drives North Atlantic Oscillation as revealed with nonlinear techniques from climatic indices

I. I. Mokhov[1] and D. A. Smirnov[2]

Received 3 September 2005; revised 19 December 2005; accepted 23 December 2005; published 7 February 2006.

[1] Based on the nonlinear techniques for estimation of coupling between oscillatory systems, we investigate the dynamics of climatic modes characterizing global and the Northern Hemisphere (NH) processes. In particular, indices of the North Atlantic Oscillation (NAO) and El Niño–Southern Oscillation (ENSO) for 1950–2004 are analyzed. The methods based on phase dynamics modeling and nonlinear "Granger causality" are used. We infer that ENSO affects NAO during the last half a century with confidence probability higher than 0.95. The influence is characterized with time delay in the range from a couple of months up to three years and increases during the last decade. **Citation:** Mokhov, I. I., and D. A. Smirnov (2006), El Niño–Southern Oscillation drives North Atlantic Oscillation as revealed with nonlinear techniques from climatic indices, *Geophys. Res. Lett.*, *33*, L03708, doi:10.1029/2005GL024557.

1. Introduction

[2] ENSO and NAO represent the leading modes of interannual climate variability for the globe and NH, respectively [*Trenberth et al.*, 1998; *Intergovernmental Panel on Climate Change*, 2001]. Different tools have been used for the analysis of their interaction, in particular, cross-correlation function (CCF) and Fourier and wavelet coherence for the sea surface temperature (SST) and sea level pressure (SLP) indices [*Wallace and Gutzler*, 1981; *Rogers*, 1984; *Pozo-Vazquez et al.*, 2001; *Jevrejeva et al.*, 2003].

[3] One often considers a NAO index defined as the normalized SLP difference between Azores and Iceland [*Rogers*, 1984] (http://www.cru.uea.ac.uk). We denote it $NAOI_{cru}$. Alternatively, NAO is characterized in [http://www.ncep.noaa.gov] as the leading decomposition mode of the field of 500 hPa geopotential height in the NH based on the "Rotated Principal Component Analysis" [*Barnston and Livezey*, 1987]. We denote it $NAOI_{ncep}$. Hence, $NAOI_{ncep}$ is a more global characteristic than $NAOI_{cru}$. ENSO indices T(Niño-3), T(Niño-3,4), T(Niño-4), T(Niño-1+2) characterize SST in the corresponding equatorial regions of the Pacific Ocean [e.g., *Mokhov et al.*, 2004]. Southern Oscillation Index (SOI) is defined as the normalized SLP difference between Tahiti and Darwin. All the signals are rather short that has made confident inference about the character of interaction difficult.

[4] New techniques for diagnostics of coupling between oscillatory systems have been developed in nonlinear dynamics during the last years to reveal complex and sufficiently weak nonlinear interactions as well as their "direction". They can be divided into two families: Estimation of interdependencies in reconstructed state spaces, [e.g., *Arnhold et al.*, 1999], and analysis of the phase dynamics [e.g., *Rosenblum and Pikovsky*, 2001]. Nonlinear methods from each family have their own conditions of superiority [*Smirnov and Andrzejak*, 2005], so that in practice it is reasonable to apply both ideas. Here, we investigate interaction between ENSO and NAO with two nonlinear techniques using several climatic indices.

2. Data and Methods

2.1. Data

[5] Mainly, we analyze the period 1950–2004 (660 monthly values). We use the indices $NAOI_{cru}$ and $NAOI_{ncep}$ for NAO and T(Niño-3,4), T(Niño-3), T(Niño-4), T(Niño-1+2), and SOI for ENSO. Longer time series for $NAOI_{cru}$ (1821–2004), T(Niño-3) (1871–1997), and SOI (1866–2004) are also considered.

2.2. Phase Dynamics Modeling

[6] The main idea is to estimate how strong future evolution of one system's phase depends on the other system's phase.

[7] First, one restores time series of the phases $\{\phi_1(t_1), \ldots, \phi_1(t_N)\}$ and $\{\phi_2(t_1), \ldots, \phi_2(t_N)\}$ from the original signals $\{x_1(t_1), \ldots, x_1(t_N)\}$ and $\{x_2(t_1), \ldots, x_2(t_N)\}$ [*Boccaletti et al.*, 2002], where N is a time series length, $t_i = i\Delta t$, $\Delta t = 1$ month in our case. We perform it with the analytic signal approach implemented via complex wavelet transform [*Lachaux et al.*, 2000]. Given a signal $X(t)$, one defines a complex analytic signal $W(t)$ as

$$W(t) = \frac{1}{\sqrt{s}} \int_{-\infty}^{\infty} X(t')\psi^*\left((t-t')/s\right)dt', \qquad (1)$$

where $\psi(\eta) = \pi^{-1/4} \exp(-j\omega_0\eta) \exp(-\eta^2/2)$ is Morlet wavelet, s is a fixed time scale. $Re\ W(t)$ can be regarded as $X(t)$ band-pass filtered with the central frequency $f \approx 1/s$ and relative bandwidth of 1/4 for $\omega_0 = 6$ used below. The phase is defined as $\phi(t) = \arg W(t)$. It is the angle of rotation of the radius-vector on the plane ($Re\ W$, $Im\ W$) which increases by 2π after each complete revolution. To avoid edge effects while estimating (1) from a time series, we ignore segments of the length 1.4 s at each edge after the phase calculation.

[1] A. M. Obukhov Institute of Atmospheric Physics, Russian Academy of Sciences, Moscow, Russia.
[2] Saratov Branch, Institute of RadioEngineering and Electronics, Russian Academy of Sciences, Saratov, Russia.

0094-8276/06/2005GL024557$05.00

[8] Second, one constructs a global model relating phase increments over a time interval τ to the phases [*Rosenblum and Pikovsky*, 2001; *Cimponeriu et al.*, 2004]

$$\begin{aligned}\phi_1(t+\tau)-\phi_1(t) &= F_1(\phi_1(t),\phi_2(t+\Delta))+\xi_1(t),\\ \phi_2(t+\tau)-\phi_2(t) &= F_2(\phi_2(t),\phi_1(t+\Delta))+\xi_2(t),\end{aligned} \tag{2}$$

where $\xi_{1,2}$ are zero-mean random processes, Δ stands for a possible time delay, F_1 is a trigonometric polynomial $F_1 = \sum_{m,n}[a_{m,n}\cos(m\phi_1 + n\phi_2) + b_{m,n}\sin(m\phi_1 + n\phi_2)]$, F_2 is defined analogously. The strength of the influence of the system 2 on the system 1 ($2 \rightarrow 1$) is quantified as

$$\begin{aligned}c_1^2 &= \frac{1}{2\pi^2}\int_0^{2\pi}\int_0^{2\pi}(\partial F_1/\partial\phi_2)^2 d\phi_1\, d\phi_2\\ &= \sum_{m,n} n^2\left(a_{m,n}^2 + b_{m,n}^2\right).\end{aligned} \tag{3}$$

The influence $1 \rightarrow 2$ is quantified "symmetrically" (c_2^2). We use the third-order polynomials for $F_{1,2}$ and set τ equal to a basic oscillation period.

[9] Given a time series, one estimates the coefficients $a_{m,n}$,$b_{m,n}$ via the least-squares routine (LSR). Then, one can get the estimate $\hat{c}_1^2$ by replacing the true values of $a_{m,n}$, $b_{m,n}$ in (3) with their estimates. A reliable detection of directional coupling can only be achieved in non-synchronous regimes. Such a situation can be diagnosed if the mean phase coherence $\rho(\Delta) = \sqrt{\langle\cos(\phi_1(t)-\phi_2(t+\Delta))\rangle_t^2 + \langle\sin(\phi_1(t)-\phi_2(t+\Delta))\rangle_t^2}$ is much less than 1. So, the approach is complementary to the synchronization analysis performed [e.g., *Maraun and Kurths*, 2005].

[10] The estimators $\hat{c}_1$ and $\hat{c}_2$ are significantly biased for short signals. Unbiased estimators γ_1 and γ_2 supplied with 95% confidence bands have been obtained by *Smirnov and Bezruchko* [2003] by introducing corrections to $\hat{c}_1^2$ and $\hat{c}_2^2$. For moderate coupling strength and phase nonlinearity, γ_1 and γ_2 guarantee that the probability of erroneously detected coupling is less than 0.025. Additional tests with exemplary oscillators show that $\gamma_1(\Delta)$ and $\gamma_2(\Delta)$ are applicable for a time series as short as 20 basic periods if $\rho(\Delta) < 0.4$. The latter condition excludes synchronous-like signals.

2.3. Nonlinear Granger Causality

[11] The technique is based on the construction of "individual" and "joint" predictors without ignoring the amplitudes of oscillations [*Feldmann and Bhattacharya*, 2004]. If the accuracy of prediction of the x_1-dynamics can be improved when some x_2-values are taken into account and not via the sophistication of an individual model then the presence of influence $2 \rightarrow 1$ is inferred. In terms of linear models, the idea was formulated already by *Granger* [1969].

[12] We normalize time series to zero mean and unit variance and construct models

$$\begin{aligned}x_1(t_n) = f_1(&x_1(t_{n-1}),\ldots,x_1(t_{n-d_1}),\\ &x_2(t_{n-1+\Delta}),\ldots,x_2(t_{n-d_2+\Delta}),\mathbf{a}),\end{aligned} \tag{4}$$

where f_1 is an algebraic polynomial of the order K, Δ is a time delay, d_1 is individual model dimension; $d_2 = 0$ for an individual model, $d_2 > 0$ for a joint one. Coefficient estimates $\hat{\mathbf{a}}$ are found via the LSR. Unbiased estimates of mean-squared prediction errors of the individual and joint models are σ_1^2 and $\sigma_{2\rightarrow1}^2$, respectively. Prediction improvement (PI) of the x_1-dynamics is quantified as $PI_{2\rightarrow1} = \sigma_1^2 - \sigma_{2\rightarrow1}^2$. Significance of the PI estimates is assessed via F-test for an appropriate statistic [e.g., *Granger*, 1969]. Everything is "symmetric" for $PI_{1\rightarrow2}$. We vary d_1, d_2, K in the range $0 \div 3$.

3. Results

3.1. Phase Dynamics Modeling

[13] Figure 1 demonstrates individual characteristics of the indices NAOI_{ncep} (Figure 1a) and T(Niño-3,4) (Figure 1d). Global wavelet spectra exhibit several peaks (Figures 1b and 1e). One can assume that they correspond to oscillatory processes for which the phase can be adequately introduced. To extract phases of "different rhythms" in NAO and ENSO, we tried several values of s in (1) corresponding to different spectral peaks. We estimated coupling between all the rhythms pairwise. The only case when substantial conclusions about the presence of coupling are inferred is the "rhythm" with $s = 32$ months for both signals, see Figures 1a and 1d. The phases are well-defined since clear rotation around the origin takes place on the complex plane shown in Figures 1c and 1f.

[14] The results of the phase dynamics modeling are shown in Figure 2 for $s = 32$ and model (2) with $\tau = 32$. Figure 2a shows that the technique is applicable only for $\Delta > -30$ where $\rho(\Delta) < 0.4$. The influence ENSO $\rightarrow$ NAO is pointwise significant for $-30 \le \Delta \le 0$ and maximal for $\Delta = -24$ months (Figure 2b). One can infer the presence of the influence ENSO $\rightarrow$ NAO as follows. Probability of a random erroneous conclusion about coupling presence based only on a pointwise significant γ_1 for a specific Δ is 0.025. Taking into account that the values of $\gamma_1(\Delta)$ separated with Δ less than τ are strongly correlated, one can consider as statistically independent the values of γ_1 from the two groups: $-30 \le \Delta \le 0$ and $0 < \Delta \le 32$. Then, the probability of erroneous conclusion based on pointwise significant γ_1 in any of the two groups is approximately twice as large, i.e., 0.05. So, from Figure 2b we conclude with confidence probability of 0.95 that the influence ENSO $\rightarrow$ NAO is present. Most probably, it is delayed by 24 months. However, the latter conclusion is not so reliable. No signs of the influence NAO $\rightarrow$ ENSO are detected (Figure 2c).

[15] Large ρ for $\Delta < -30$ does not imply strong coupling. For such short time series and close basic frequencies of oscillators, the probability to get $\rho > 0.4$ for uncoupled processes is greater than 0.5 as observed in numerical experiments with exemplary oscillators.

[16] All the reported results remain the same for any s in the range $29 \div 34$ months and relative bandwidth $0.2 \div 0.4$. Phase calculation based on band-pass filtering and Hilbert transform leads to similar results, for example, for the 2-nd order Butterworth filter and the same bandwidth.

[17] The use of other ENSO indices instead of T(Niño-3,4) gives almost the same results as in Figure 2.

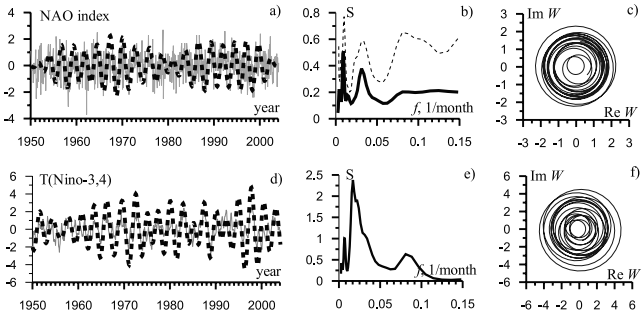

Figure 1. Characteristics of $NAOI_{ncep}$ and T(Niño-3,4). (a) $NAOI_{ncep}$ (gray line) and *Re W* for $s = 32$ months (dashed line). (b) Global wavelet spectrum of $NAOI_{ncep}$ (solid line) and $NAOI_{cru}$ for the period 1950–2004 (dashed line). (c) An orbit $W(t)$ for $NAOI_{ncep}$, $s = 32$ months. (d)–(f) The same as Figures 1a–1c for T(Niño-3,4).

Only for T(Niño-1+2), coupling is not so pronounced. Analysis of other rhythms in $NAOI_{ncep}$ and T(Niño-3,4) does not lead to significant conclusions about the presence of interaction.

[18] For $NAOI_{cru}$ the width of the peak corresponding to $s = 32$ months is greater than for $NAOI_{ncep}$, Figure 1b. It leads to stronger phase diffusion of the 32-month rhythm as quantified by mean-squared residual errors in the estimation of equation (2) [*Smirnov and Andrzejak*, 2005]. As a result, we have not observed significant coupling between $NAOI_{cru}$ and any of the ENSO indices for the period 1950–2004 as well as for the longer recordings (1871–1997, 1866–2004).

3.2. Nonlinear Granger Causality

[19] CCF values for the pair $NAOI_{ncep}$ – T(Niño-3,4) are not pointwise significant at $p < 0.05$. Analysis of the nonlinear Granger causality for the models (4) with $d_2 = 1$,

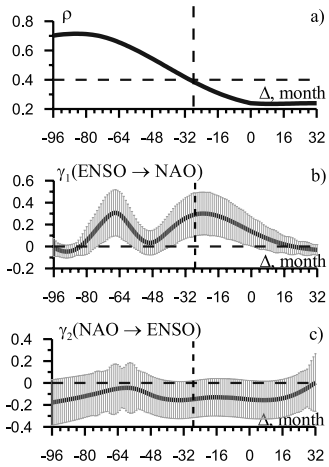

Figure 2. Coupling between $NAOI_{ncep}$ and T(Niño-3,4) (1950–2004) in terms of the phase dynamics. (a) Mean phase coherence. (b) and (c) Strengths of the influence ENSO → NAO and NAO → ENSO, respectively, with their 95% confidence bands.

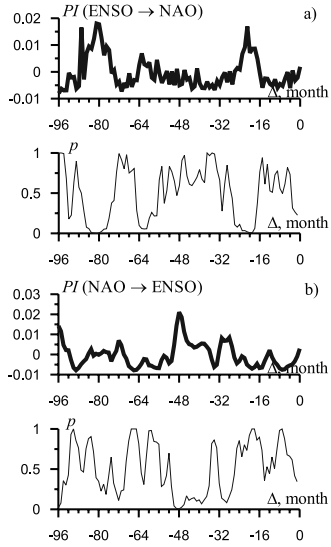

Figure 3. Coupling between $NAOI_{ncep}$ and T(Niño-3,4) (1950–2004) in terms of the nonlinear Granger causality. (a) PI of $NAOI_{ncep}$, (b) PI of T(Niño-3,4). Pointwise p-level is shown below each panel.

$K = 2$ gives more interesting results. For the simplest case of $d_1 = 0$ Figure 3a shows that PI of NAO is about 1.5–2% for the time delays $\Delta = -(19 \div 21)$ or $\Delta = -(80 \div 83)$ months. Each of those PI-values is pointwise significant at $p < 0.01$. Taking into account strong correlations of $PI_{ENSO \rightarrow NAO}$ separated with Δ less than 4, one can infer that the influence ENSO → NAO is present at $p < 0.05$. Single pointwise significant PI of ENSO for $\Delta = -(48 \div 49)$ months (Figure 3b) does not allow confident conclusion about the presence of the influence NAO → ENSO.

[20] For d_1 and d_2 increased up to 2, no changes in PI values presented in Figure 3 are observed. So, the reported PI is not achieved via complication of the individual model. Simultaneous increase in d_1 up to 3, K up to 3, and d_2 up to 2 leads to the absence of any confident conclusions due to large variance of the estimators.

[21] Similar results are observed if T(Niño-3,4) is replaced with T(Niño-3), T(Niño-4), or SOI. However, the conclusion about the presence of the influence ENSO → NAO becomes less confident ($p < 0.1$). The use of T(Niño-1+2) leads to even less significant results. Analogously to phase dynamics modeling, replacement of $NAOI_{ncep}$ with $NAOI_{cru}$ does not lead to reliable coupling detection neither for the period 1950–2004 nor for longer periods.

[22] Finally, to reveal trends in coupling during the last decade, we estimated coupling between $NAOI_{ncep}$ and T(Niño-3,4) in a moving window of the length of 47 years. We started with the interval 1950–1996 and finished with 1958–2004. PI-values reveal increase in the strength of the influence ENSO → NAO. The value of $PI_{ENSO \rightarrow NAO}$ for $\Delta = -(19 \div 20)$ months rises almost monotonously by 150% (Figure 4). Although it is difficult to assess statistical significance of the conclusion, the monotone character of the increase indicates that it can hardly be an effect of

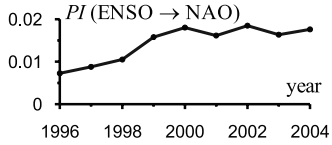

Figure 4. Influence ENSO → NAO for $NAOI_{ncep}$ and T(Niño-3,4) in a 47-year moving window. Max{$PI_{ENSO\rightarrow NAO}(\Delta = -19)$, $PI_{ENSO\rightarrow NAO}(\Delta = -20)$} is shown versus the last year of the moving window.

random fluctuations. To a certain extent, it can be attributed to the strong 1997–98 ENSO event.

4. Conclusions

[23] The presence of coupling between ENSO and NAO is revealed with the use of two nonlinear techniques and different climatic indices. Consistent results are observed in all cases. The influence ENSO → NAO is detected with confidence probability of 0.95 with the use of $NAOI_{ncep}$ (1950–2004). Estimates of the time delay in the influence range from a couple of months up to three years with the most probable value of 20–24 months. Besides, increase in the strength of the influence during the last decade is observed. Possible physical mechanisms underlying oscillations and interactions as slow and even slower than reported here are considered [e.g., *Latif*, 2001; *Pozo-Vazquez et al.*, 2001; *Jevrejeva et al.*, 2003].

[24] The influence ENSO → NAO is not detected with the use of $NAOI_{cru}$ due to different properties of this "more local" than $NAOI_{ncep}$ index.

[25] Backward influence NAO → ENSO is not detected with confidence for any indices.

[26] **Acknowledgment.** The work was supported by the RFBR (grants 05-02-16305, 05-05-64907, 04-05-08063-ofi-a), Russian Science Support Foundation, the President of Russia (grants MK-1067.2004.2, Scientific Schools-1636.2003.5), RAS, and BRHE Program (REC-006).

References

Arnhold, J., K. Lehnertz, P. Grassberger, and C. E. Elger (1999), A robust method for detecting interdependences: Application to intracranially recorded EEG, *Physica D*, *134*, 419.

Barnston, A. G., and R. E. Livezey (1987), Classification, seasonality, and persistence of low frequency atmospheric circulation patterns, *Mon. Weather Rev.*, *115*, 1083.

Boccaletti, S., et al. (2002), The synchronization of chaotic systems, *Phys. Rep.*, *366*, 1.

Cimponeriu, L., M. Rosenblum, and A. Pikovsky (2004), Estimation of delay in coupling from time series, *Phys. Rev. E*, *70*, 046213, doi:10.1103/PhysRevE.70.046213.

Feldmann, U., and J. Bhattacharya (2004), Predictability improvement as an asymmetrical measure of interdependence in bivariate time series, *Int. J. Bifurcation Chaos*, *14*, 505.

Granger, C. W. J. (1969), Investigating causal relations by econometric models and cross-spectral methods, *Econometrica*, *37*, 424.

Intergovernmental Panel on Climate Change (IPCC) (2001), *Climate Change 2001: The Scientific Basis: Contribution of Working Group I to the Third Assessment Report of the Intergovernmental Panel on Climate Change*, edited by J. T. Houghton et al., 881 pp., Cambridge Univ. Press, New York.

Jevrejeva, S., J. Moore, and A. Grinsted (2003), Influence of the Arctic Oscillation and El Niño–Southern Oscillation (ENSO) on ice conditions in the Baltic Sea: The wavelet approach, *J. Geophys. Res.*, *108*(D21), 4677, doi:10.1029/2003JD003417.

Lachaux, J. P., E. Rodriguez, M. Le Van Quyen, A. Lutz, J. Martienerie, and F. J. Varela (2000), Studying single-trials of phase synchronous activity in the brain, *Int. J. Bifurcation Chaos*, *10*, 2429.

Latif, M. (2001), Tropical Pacific/Atlantic Ocean interactions at multi-decadal time scales, *Geophys. Res. Lett.*, *28*, 539–542.

Maraun, D., and J. Kurths (2005), Epochs of phase coherence between El Niño/Southern Oscillation and Indian monsoon, *Geophys. Res. Lett.*, *32*, L15709, doi:10.1029/2005GL023225.

Mokhov, I. I., D. V. Khvorostyanov, and A. V. Eliseev (2004), Decadal and longer term changes in El Niño–Southern Oscillation characteristics, *Int. J. Clim.*, *24*, 401.

Pozo-Vazquez, D., M. J. Esteban-Parra, F. S. Rodrigo, and Y. Castro-Diez (2001), The association between ENSO and winter atmospheric circulation and temperature in the North Atlantic region, *J. Clim.*, *14*, 3408.

Rogers, J. C. (1984), The association between the North Atlantic Oscillation and the Southern Oscillation in the North Hemisphere, *Mon. Weather Rev.*, *112*, 1999.

Rosenblum, M. G., and A. S. Pikovsky (2001), Detecting direction of coupling in interacting oscillators, *Phys. Rev. E*, *64*, 045202, doi:10.1103/PhysRevE.64.045202.

Smirnov, D. A., and R. G. Andrzejak (2005), Detection of weak directional coupling: Phase-dynamics approach versus state-space approach, *Phys. Rev. E*, *71*, 036207, doi:10.1103/PhysRevE.71.036207.

Smirnov, D. A., and B. P. Bezruchko (2003), Estimation of interaction strength and direction from short and noisy time series, *Phys. Rev. E*, *68*, 046209, doi:10.1103/PhysRevE.68.046209.

Trenberth, K. E., et al. (1998) CLIVAR Initial Implementation Plan, *WCRP 103*, 313 pp., World Clim. Res. Program, Geneva, Switzerland. (Available at http://www.clivar.org/publications/other_pubs/iplan/climp.htm.)

Wallace, J. M., and D. S. Gutzler (1981), Teleconnections in the geopotential height field during the Northern Hemisphere winter, *Mon. Weather Rev.*, *109*, 784.

I. I. Mokhov, A. M. Obukhov Institute of Atmospheric Physics, Russian Academy of Sciences, 3 Pyzhevsky, Moscow 119017, Russia. (mokhov@ifaran.ru)

D. A. Smirnov, Saratov Branch, Institute of RadioEngineering and Electronics, Russian Academy of Sciences, 38 Zelyonaya Street, Saratov 410019, Russia. (smirnovda@info.sgu.ru)